Surface instability and possible polymerization in RbH_2PO_4 at high temperatures

1998 J. Phys.: Condens. Matter 10 9593

(http://iopscience.iop.org/0953-8984/10/43/002)

J. Phys.: Condens. Matter **10** (1998) 9593–9607. Printed in the UK PII: S0953-8984(98)92650-9

Surface instability and possible polymerization in RbH_2PO_4 at high temperatures

Jong-Ho Park†, Kwang-Sei Lee‡§ and Jung-Nam Kim†

† Department of Physics, Pusan National University, Pusan 609-735, Korea

‡ Department of Physics, Inje University, Kimhae 621-749, Kyungnam, Korea

Received 17 March 1998, in final form 25 August 1998

Abstract. We have investigated in detail the high-temperature phenomena of RbH_2PO_4 by means of optical microscopy, differential scanning calorimetry (DSC), and impedance spectroscopy. The so-called high-temperature transformation temperature T_p is scattered widely over the temperature range of 82–117 °C, depending strongly upon the experimental conditions such as sample quality and experimental probes. It has been observed by thermomicroscopy that, upon heating above 110 °C, the cracks appeared at the surface and the crack pattern grew up with increasing temperature above 110 °C, and on suitable prolonged heat treatment at constant temperature near 110 °C. The activation energy is estimated from DSC, which revealed the wide scatter of T_p over the range 82–117 °C. The complex ac impedance spectra near 113 °C were fitted by superposition of two Cole–Cole types of relaxations. The fast component is interpreted as proton migration in the bulk, while the slow component is accounted for as a cluster formation due to breaking and reforming of the hydrogen bond at the surface.

Our results show evidence that the high-temperature phenomenon of RbH_2PO_4 near T_p is not a polymorphic structural phase transition of the tetragonal phase to a presumed monoclinic modification, but a slow partial polymerization of RbH_2PO_4 into $Rb_nH_2P_nO_{3n+1}$ (probably $n = 2$) at reaction sites at the surface of crystal. The high-temperature phenomenon is believed to be controlled by the topochemical factors.

1. Introduction

The low-temperature ferroelectric phase transition at −126 °C (T_c) in the RbH_2PO_4 crystal has been investigated for a long time [1]. The high-temperature transformation of RbH_2PO_4 near T_p has also been studied by a number of workers [2–22], but the T_p is scattered more widely over the temperature range of 72–130 °C than one would expect and there are considerable differences in the published reports concerning the high-temperature behaviour. Therefore, it is inconclusive whether it is a high-temperature phase transition (HTPT) or thermal decomposition.

Most investigators have considered the high-temperature anomaly of RbH_2PO_4 near T_p as a structural phase transition, because weight loss of bulk samples of more than 0.1 wt% in thermogravimetry (TG) data could be detected near 150 °C [3, 5, 9], higher than the reported T_p range (72–130 °C) [2–22]. The high-temperature phenomena have been reported by measurements of thermal analyses [2–14], optical observation [4, 6, 19], x-ray diffraction

§ Author to whom correspondence should be addressed. E-mail: kslee@physics.inje.ac.kr.

0953-8984/98/439593+15$19.50

[4, 6, 14], dielectric constant [15, 17], Raman scattering [18], electrical conductivity [17, 19], infrared reflectivity [4, 16, 17, 20], and nuclear magnetic resonance (NMR) and nuclear quadrupole resonance (NQR) [4, 21]. The high-temperature transformation is indicated as one endothermic peak on the differential thermal analysis (DTA) curve at 120 [2, 3], 100 [4], 90 [8], or 130 °C [9], or as two endothermic peaks in the differential scanning calorimetry (DSC) curve at 93 and 115 °C [6] or 79 and 107 °C [13]. Pereverzeva *et al* reported two anomalies at 30 and 125 °C by dielectric constant measurements [15]. Shapira *et al* reported that the high-temperature transformation temperature varies between 72 and 102 °C, depending strongly on crystalline perfection [17]. Blinc *et al* observed a high-temperature anomaly near 86 °C in NMR and NQR measurements [4, 21]. D'yakov *et al* insisted that the supercooled metastable high-temperature phase (previously proposed as a monoclinic system) transforms back to the original tetragonal phase, but transformation rate is strongly dependent on the surrounding moisture [6]. Baranowski *et al* studied the effect of grinding, one-dimensional pressing or contact with appropriate water vapour pressure on the supercooled crystal [10, 11, 12], and they concluded that the presence of adsorbed water is essential for the removal of the metastability of the supercooled high-temperature phase.

However, the same DTA, DSC and TG data in the same temperature range might be interpreted as a consequence of thermal decomposition. Under non-equilibrium conditions, dehydration in the bulk of RbH_2PO_4 takes place in the temperature range 200–600 °C with the formation of rubidium dihydrogen pyrophosphate ($Rb_2H_2P_2O_7$) and rubidium polyphosphate ($Rb_nH_2P_nO_{3n+1}$ ($n \gg 1$) $\simeq$ $(RbPO_3)_n$) as intermediate and final products, respectively [2, 3, 4, 6, 7, 9]. Under equilibrium conditions, the reaction takes place in two stages in the temperature range 150–200 °C with the loss of 0.5 water molecules at each stage [5]. According to these chemical analyses [2–9], it is believed that the stoichiometry of bulk crystals above 150 °C starts to deviate appreciably from the chemical formula RbH_2PO_4. However, recent TG and DSC studies of RbH_2PO_4 by Ortiz *et al* [14] showed, in contrast to many published results, the existence of a small but distinct amount of water weight loss related to the high-temperature transformation around 116 °C.

The condensation of phosphates has been the subject of much investigation in crystal chemistry and a few excellent reviews have already appeared [23, 24, 25], so that Lee proposed that the thermal condensation such as the following chemical reaction:

$$n\mathrm{MH_2PO_4\ (s)} \rightarrow \mathrm{M}_n\mathrm{H_2P}_n\mathrm{O}_{3n+1}\ \mathrm{(s)} + (n-1)\mathrm{H_2O\ (v)} \qquad (1)$$

sets in around T_p (see figure 5 of [26] for a realistic phase interrelationship of KH_2PO_4 and RbH_2PO_4 and their polymer products), where n is the number of molecules participating in thermal decomposition (condensation polymerization) [26]. The letters s and v enclosed in parentheses denote that the corresponding compound is in the solid or vapour state. Chain-like polyphosphates, ring-like metaphosphates and cross-linked ultraphosphates may be formed [23, 26]. Lee claimed that the high-temperature anomaly should be interpreted as an *onset of partial polymerization at reaction sites at the surface of solids* (see figure 7 in [26]). A similar high-temperature phenomenon has been much studied in KH_2PO_4 around T_p (170–225 °C) [7, 14, 19, 22, 27, 28, 29, 30], but recent experimental results verified the evidence of a chemical reaction of the type in (1) at the surface rather than polymorphic structural phase transition [14, 28, 29, 30]. Therefore, referring to the similar natures of the high-temperature phenomena of RbH_2PO_4 and KH_2PO_4, there still remains a question whether the high-temperature anomaly of RbH_2PO_4 is a structural phase transition or thermal decomposition. Moreover, it is not known as yet whether or not the so-called high-temperature phase of RbH_2PO_4 and that of KH_2PO_4 are the same, although many investigators have assumed the monoclinic crystal system above T_p [26]. Therefore, we

investigated the high-temperature anomaly of RbH_2PO_4 by means of optical microscopy, DSC, and impedance spectroscopy.

2. Experimental details

Single crystals of RbH_2PO_4 were grown from aqueous solution at 45 °C by slow evaporation of the solvent. Thermal and dielectric properties were investigated for samples grown in the same crystallizer. The samples were neither annealed nor submitted to any thermal treatments before the measurement, but they were mechanically treated (grinding and polishing for the optical observation and for ohmic contact of electrode). Optical observation was carried out by means of a polarizing microscope (Olympus BH-2). Specimens were illuminated by transmission light along the *c* axis. The DSC study was performed in the temperature range from 30 to 300 °C by using a Dupont 910 differential scanning calorimeter in ambient atmosphere. The single crystals were finely crushed (without grinding) and were used in the DSC experiment. The complex ac impedance, $Z^*(\omega)$, was measured between 100 Hz and 10 MHz by using an impedance/gain-phase analyser (HP 4194A). The experiments were performed between 30 and 200 °C in ambient atmosphere and the temperature of the sample was measured with a platinum–rhodium thermocouple. The heating rate was 0.2 °C min^{-1}.

3. Results and discussion

3.1. Optical microscopy

In order to clarify that the high-temperature transformation of RbH_2PO_4 around T_p is due to the cooperative phenomenon or due to the partial thermal decomposition, optical observation was made by using a polarizing microscope. At first we tried to observe the change of birefringence at high temperatures under the crossed polarizers, but failed to see any domain-like pattern. Therefore, we used the unpolarized light over the whole temperature range. Figures 1(a)–(d) are microscope photographs of the surface of the RbH_2PO_4 crystal along the *c* axis. On heating at a rate of 10 °C min^{-1}, a few cracks appeared abruptly at the surface of RbH_2PO_4 near 112 °C. These cracks became more evident, and then intensive cracking sets in, making the crystal completely opaque. The onset of cracking was strongly dependent on both sample quality and the heating rate, in agreement with [6]. The cracks appeared at higher temperatures in the thinner samples, indicating that the thinner samples can accommodate the higher strains induced by the high-temperature transformation. This observation suggests that the high-temperature transformation of RbH_2PO_4 is controlled by topochemical factors. Figures 2(a)–(d) show the appearance of cracks and their temporal evolution under the isothermal condition at 109 °C. On tempering at a constant temperature of 109 °C, the crack patterns grew and merged together. Recently, Park *et al* reported that the microcracks appeared at the surface of KH_2PO_4 near 210 °C [30]. Therefore, the appearance of cracks near 110 °C in RbH_2PO_4 is similar to that near 180 °C in KH_2PO_4.

The appearance of microcracks upon heating above T_p has already been observed [4, 6, 19, 30]. After prolonged heat treatment near T_p, the sample changes from being transparent and colourless to milky white. According to Lee's interpretation [26], the microscopic origin of cracks results from hydrogen-bond breaking due to the thermal decomposition of (1). As the temperature rises above T_p or the sample is tempered at constant temperature above T_p, the more monomers react and dehydration may start at

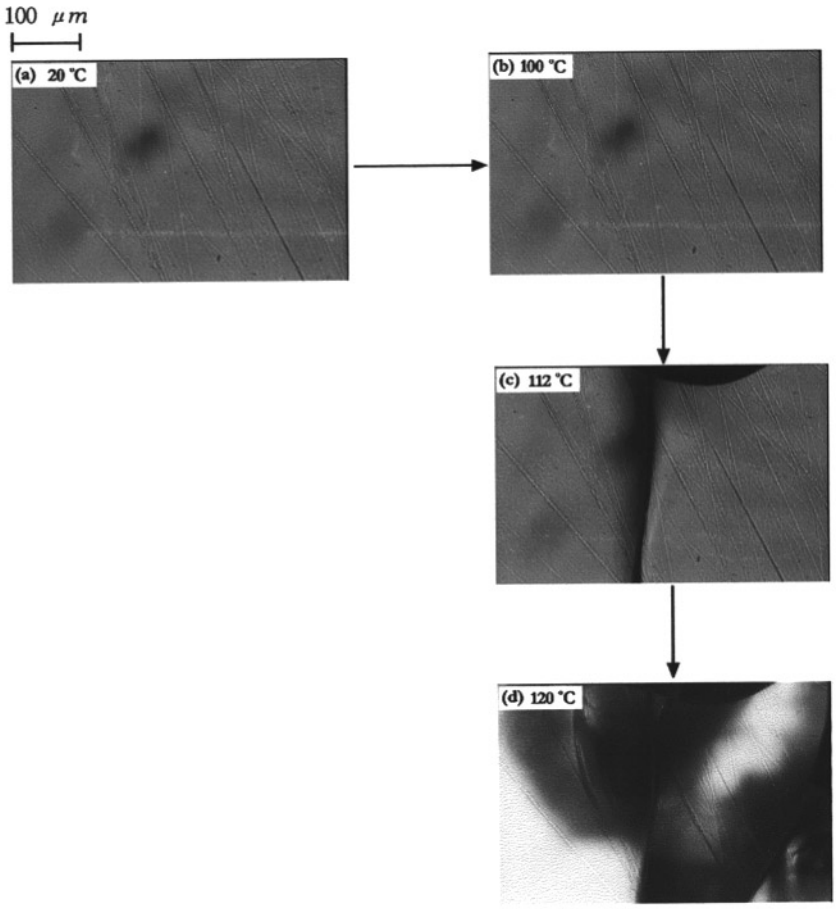

Figure 1. Effect of temperature on the surface morphology of RbH_2PO_4 along the *c* axis at (a) 20, (b) 100, (c) 112 and (d) 120 °C (heating rate: 10 °C min^{-1}).

reaction sites distributed on the surface of solids. As H_2O molecules are formed at or near the surface, the increased water vapour pressure can render the surface microcracked. However, the internal stress field results from defects such as dislocations, vacancies, interstitials, impurity atoms of the alloying elements, segregations and particles embedded in the matrix. These imperfections distort the crystal lattice: a stress field surrounds the crystal defect. These defect sites may be the starting points of thermal decomposition. Its kinetic process can be understood in terms of *nucleation and growth of cracks* according to chemical reactions such as (1). Numerous observations confirm that decomposition of solid reactants is in general initiated at defective regions of the crystal such as the surface, or more specifically, points of emergence of dislocations at the surface [31, 32]. Likewise, nuclei of the solid product $Rb_nH_2P_nO_{3n+1}$ can be thus formed, the gaseous product escapes and the resulting disruption causes strain in the neighbouring regions of unreacted RbH_2PO_4. The present interpretation is similar to the cases of surface transformation in TlH_2PO_4 [33] and $(NH_4)_2SO_4$ [34, 35] crystals, but the appearance of cracks in RbH_2PO_4 differs from that of pores in TlH_2PO_4 and $(NH_4)_2SO_4$.

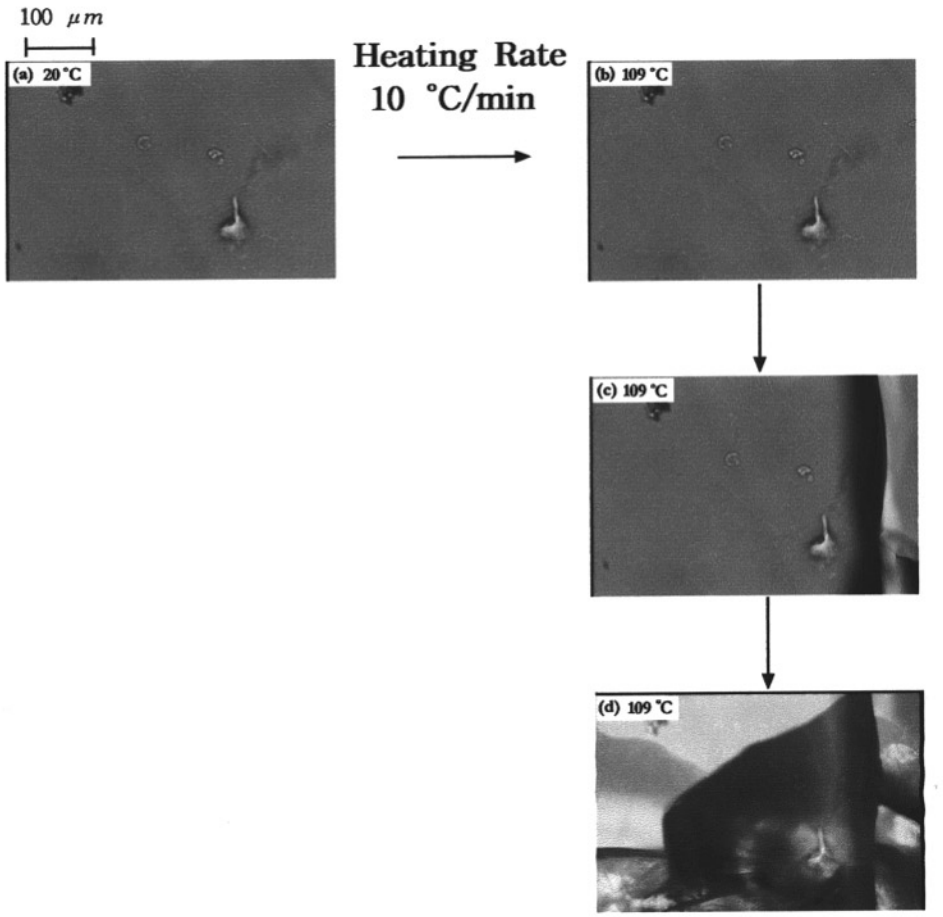

Figure 2. Temporal evolution of surface morphology of RbH_2PO_4 along the *c* axis at (a) 20 °C, (b) 109 °C after heating at a rate of 10 °C min^{-1}, (c) 109 °C after tempering for 150 min, and (d) 109 °C after tempering for 5 min when the first crack appeared in (c).

3.2. Differential scanning calorimetry (DSC)

The DSC experiment was performed with various heating rates of 2, 5, 8, 10, 15 °C min^{-1} in ambient atmosphere. As shown in figure 3, the transformation temperature (T_p) corresponding to the peak of DSC signals depended strongly on the heating rates. The thermal transformation which appears at temperatures between 82 and 117 °C is one endothermic peak for crushed (without grinding) small pieces of single crystals, while two endothermic peaks were occasionally detected for powder (finely ground) samples. It may be due to the enthalpy change caused by thermal decomposition of RbH_2PO_4 at the surface. The slower the heating rate, the lower the onset temperature of thermal transformation. This is obvious for the case of the first-order phase transition under nonequilibrium conditions or for the case of chemical reaction. The present result is believed to belong to the latter case. The slower heating rate means that the time (Δt) which is needed for the system to reach the chemical equilibrium at a given temperature is sufficient. Therefore, the decomposition

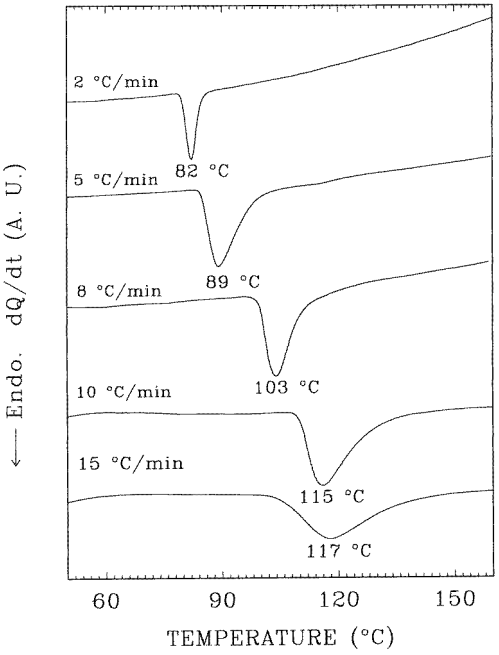

Figure 3. Influence of the heating rates on the DSC curves of RbH_2PO_4.

reaction begins to occur at lower temperatures as Δt increases.

In order to derive the activation energy which is required for high-temperature transformation near T_p, the well-known methods of Kissinger and Ozawa are used. Kissinger [36] suggested that the activation energy of a first-order process may be estimated from the variation of the temperature of maximum intensity of the DTA peak with various heating rates. The kinetics of the thermal decomposition of volatile products can be described by the following equation [37]

$$\frac{\mathrm{d}x}{\mathrm{d}t} = Dx^b \tag{2}$$

where $D = A\exp(-E/k_BT)$, x $(0 \leqslant x \leqslant 1)$ is the volume fraction of the sample that has not yet reached final chemical equilibrium, b is the order of the kinetics, E is the activation energy, k_B is Boltzmann's constant and A is the pre-exponential factor. Assuming first-order kinetics ($b = 1$) gives

$$\frac{\mathrm{d}x}{\mathrm{d}t} = \frac{A}{\phi}x\exp(-E/k_BT_p) \tag{3}$$

where $\phi = \mathrm{d}T/\mathrm{d}t$ is the heating rate. Assuming the heating rate to be constant and setting $\mathrm{d}^2x/\mathrm{d}T^2 = 0$ gives

$$E/k_BT_p^2 = \frac{A}{\phi}\exp(-E/k_BT_p). \tag{4}$$

Differentiating (4) gives

$$\frac{\mathrm{d}(\ln(\phi/T_p^2))}{\mathrm{d}(1/T_p)} = -\frac{E}{k_B}. \tag{5}$$

Thus, plotting $\ln(\phi/T_p^2)$ versus $1/T_p$ gives a slope equal to $-E/k_B$. Therefore, the activation energy can be obtained.

On the other hand, Ozawa [38] proposed that the activation energy may be estimated by shifting the DSC curve as the heating rate is changed. It is based on the general equation

$$\frac{\mathrm{d}x}{\mathrm{d}t} = Af(x)\exp(-E/k_BT) \tag{6}$$

where $f(x)$ can be a general function of x. The integration of (6), assuming a constant heating rate, gives

$$\int_{x_0}^{x} \frac{\mathrm{d}x}{f(x)} = \frac{A}{\phi}\int_{T_0}^{T} \exp(-E/k_BT)\mathrm{d}T. \tag{7}$$

Taking $\int_0^T \exp(-E/k_BT)\mathrm{d}T = (E/k_B)p\exp(E/k_BT)$ and assuming $E/k_BT > 20$ can be approximated by the following formula, where p is the Doyle's p function [37]

$$\ln p(E/k_BT) = -2.315 - 0.4567E/k_BT. \tag{8}$$

The left hand side of (7) does not depend on the heating rate. Therefore, from (8) the following linear relation for a given value of x is derived

$$\ln\phi + 0.4567E/k_BT = \text{constant}. \tag{9}$$

Thus plotting $\ln\phi$ versus $1/T_p$ gives a slope equal to $-0.4567E/k_B$.

Therefore, the activation energy can be obtained. The main basis of Kissinger's method is that the peak temperature in the DTA signal is the temperature at which the reaction rate is a maximum. This assumption has been shown to be incorrect; the maximum rate of reaction occurs somewhere before this point. Ozawa concludes that Kissinger's assumption is valid for DSC curves because of their derivative nature. Therefore, the activation energies of the thermal transformation were obtained by DSC data using Ozawa's method, and the values compared with those of Kissinger's method. The activation energies are shown in figure 4.

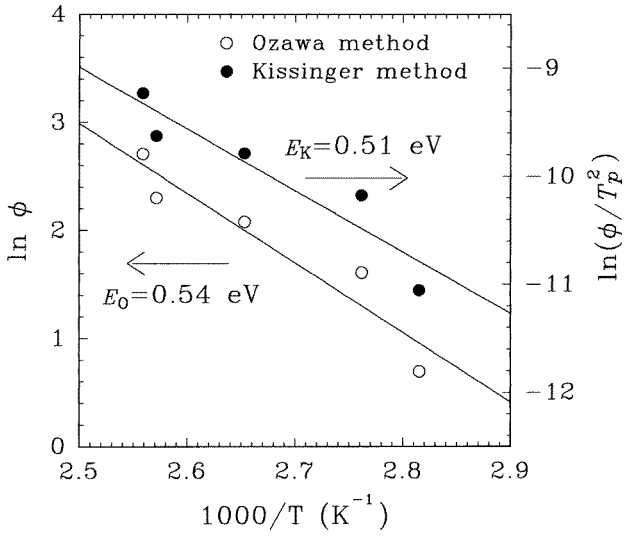

Figure 4. The plots by the methods of Kissinger and Ozawa. The solid lines represent fits to equations (5) and (9).

The activation energies estimated are E_K = 0.51 eV for Kissinger's method and E_O = 0.54 eV for Ozawa's method. The activation energy obtained by Ozawa's method is 0.03 eV higher than that obtained using Kissinger's method. We believe that the activation energy ($\sim$ 0.52 eV) obtained here is caused by the condensation of RbH_2PO_4 into $Rb_nH_2P_nO_{3n+1}$ (probably a low degree of polymerization, e.g., $n = 2$ dimers) at the surface, that is to say, polymerization via dehydration with weight loss less than 0.1 wt%.

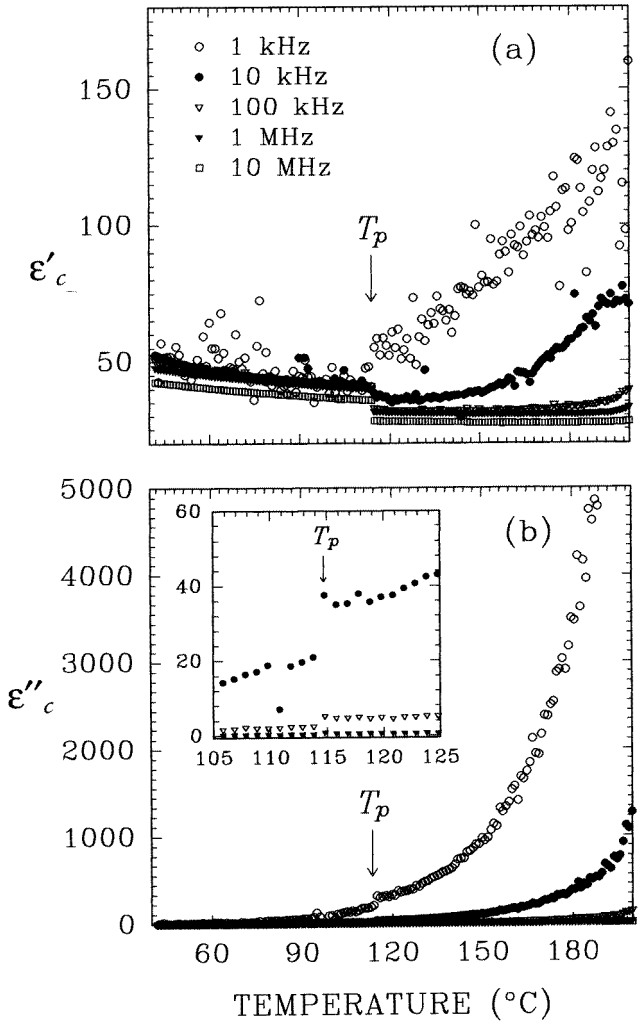

Figure 5. Temperature dependence of (a) (ε_c') and (b) (ε_c'') of the complex dielectric constant of RbH_2PO_4 at various frequencies. Heating rate: 0.2 °C min^{-1}.

3.3. Impedance spectroscopy

If upon heating RbH_2PO_4 above T_p the decomposition begins to take place at reaction sites on the surface of crystals [26, 31, 32], the space charge due to the formation of a surface layer will be reflected in the impedance measurement. Therefore, impedance spectroscopy

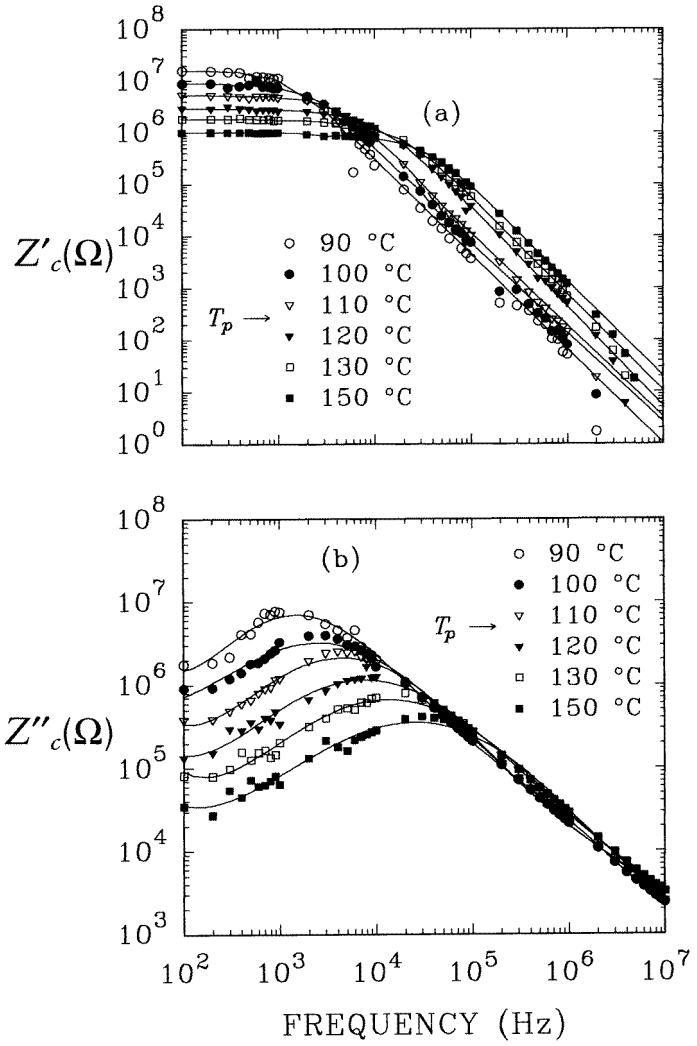

Figure 6. Impedance spectra of (a) Z'_c and (b) Z''_c in RbH_2PO_4. The solid line represents a fit to equation (10).

is a much more sensitive probe, compared with optical microscopy or DSC. Figures 5(a) and (b) show the real (ε'_c) and imaginary (ε''_c) parts of the complex dielectric constant along the *c* axis, in the temperature range between 30 and 190 °C at several frequencies with measuring temperature interval 1.0 ± 0.1 °C. The heating rate was about 0.2 °C min^{-1}, much slower than the rates for optical microscopy and DSC. The dielectric constant along the *c* axis for a certain sample, ε'_c decreases slightly with increasing temperature and then it drops discontinuously around 113 °C (T_p) for all frequencies. The value of ε'_c is almost independent of frequency up to 10 MHz at temperatures below 113 °C. The discontinuous change of ε'_c is similar to results reported previously [17]. The value of ε''_c increases gradually to 113 °C and then increases rapidly with further heating. It is well known that ε'' is related to the ionic conductivity σ as $\varepsilon_0\omega\varepsilon'' = \sigma$, where ω is the frequency of the applied

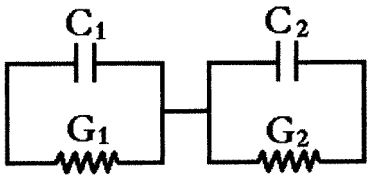

Figure 7. Equivalent circuit proposed for description of high-temperature behaviour of RbH_2PO_4.

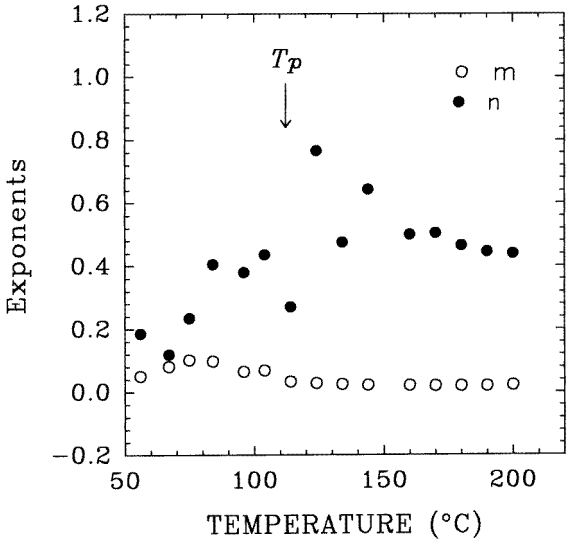

Figure 8. Temperature dependence of exponents m and n in RbH_2PO_4 along the c axis.

field and ε_0 the vacuum permittivity [39]. As shown in figure 5(b), ε_c'' increases gradually because the electrical conductivity increases on heating above room temperature. According to Schmidt [40], proton intrabond transfer in O–H···O bonds is the mechanism for dynamic behaviour of rubidium/ammonium dihydrogen phosphate mixed crystals. Because of strong proton–proton interaction, such transfer is associated with thermally activated creation of H_3PO_4 and HPO_4 intrinsic Takagi defects, their hindered diffusion in a random-step fractal potential, and their eventual annihilation. The orientational defects, D (two hydrogens within the same O···O distance) or L (lack of hydrogen), are proposed [22]. They are formed thermally in pairs by interbond jumping between different O–H···O bonds, but migrate individually. Proton conduction is thus expected to be related to the presence of defects such as the H_3PO_4 and HPO_4 ionization defects and/or D or L defects. The intrabond and interbond jumps may be dominant on approaching the T_p of thermal decomposition of the RbH_2PO_4 crystal at the surface.

According to Shapira *et al* [17], T_p is found to vary over the range of 72–102 °C being strongly dependent on the source of the specimen. The wide scatter of T_p was also confirmed in our dielectric constant measurements of a few samples, the reason for which may be the different distribution of defects at the surface from crystal to crystal. This reveals indirectly the inherent tendency to thermal decomposition of crystals, accompanied by dehydration at the surface and the topochemical nature of the high-temperature phenomenon around

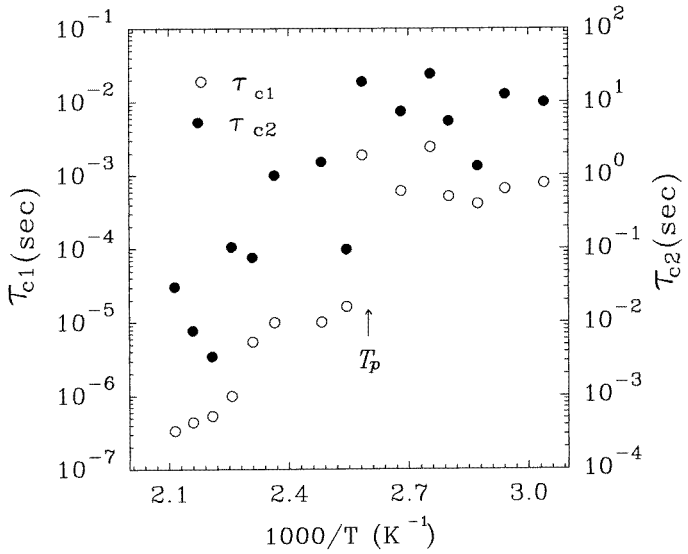

Figure 9. Temperature dependence of relaxation time τ_{c1} and τ_{c2} on $1/T$ in RbH_2PO_4.

T_p [31].

Figures 6(a) and (b) present the variation of the real (Z_c') and the imaginary (Z_c'') part of the impedance versus frequency using a double logarithmic scale for several temperatures. It is observed that, above as well as below T_p, the Z_c' in the high-frequency region decreases slowly from 10^4 to 10^6 Hz, depending on the temperature and then continuously decreases with an increasing frequency of approximately $1/\omega$ near the relaxation frequency. The relaxational peak frequency of Z_c'' moves to a high-frequency region with increasing temperature. The absolute values of the high-frequency slopes are, in fact, very close to unity and seem to be independent of the temperature while the low-frequency slopes have values lower than unity and are strongly temperature dependent. These two different tendencies in the temperature dependence suggest that two dispersion mechanisms must be involved. Considering the existence of two dispersion mechanisms and the bulk conductance G_1 and the surface conductance G_2 of the material, an equivalent circuit can be proposed, as shown in figure 7 [28, 39]. The overall impedance spectra of RbH_2PO_4 are similar to that reported previously for KH_2PO_4 [27, 28].

Therefore, impedance spectra of RbH_2PO_4 can be analysed by the same method applied to KH_2PO_4 [28]. The complex impedance of material with two independent relaxators characterized by relaxation times τ_{c1} and τ_{c2} may be written in the superposition of the two Cole–Cole expressions:

$$Z^*(\omega) = \frac{1/G_1}{1 + (\mathrm{i}\omega\tau_{c1})^{1-m}} + \frac{1/G_2}{1 + (\mathrm{i}\omega\tau_{c2})^{1-n}} \tag{10}$$

where $\tau_{c1} = 1/\omega_{p1}$, $\tau_{c2} = 1/\omega_{p2}$, and ω_{p1} and ω_{p2} are the characteristic angular frequencies. The solid lines in figure 6(b) are theoretical curves obtained by using (10). Only the data relevant to the imaginary part were used in the fitting. The six parameters obtained, G_1, G_2, τ_{c1}, τ_{c2}, m, and n, were then introduced into the real part of the formula to check whether the calculated values are also in agreement with the measured value of Z_c'. The agreement between experimental and calculated values for both real and imaginary parts of

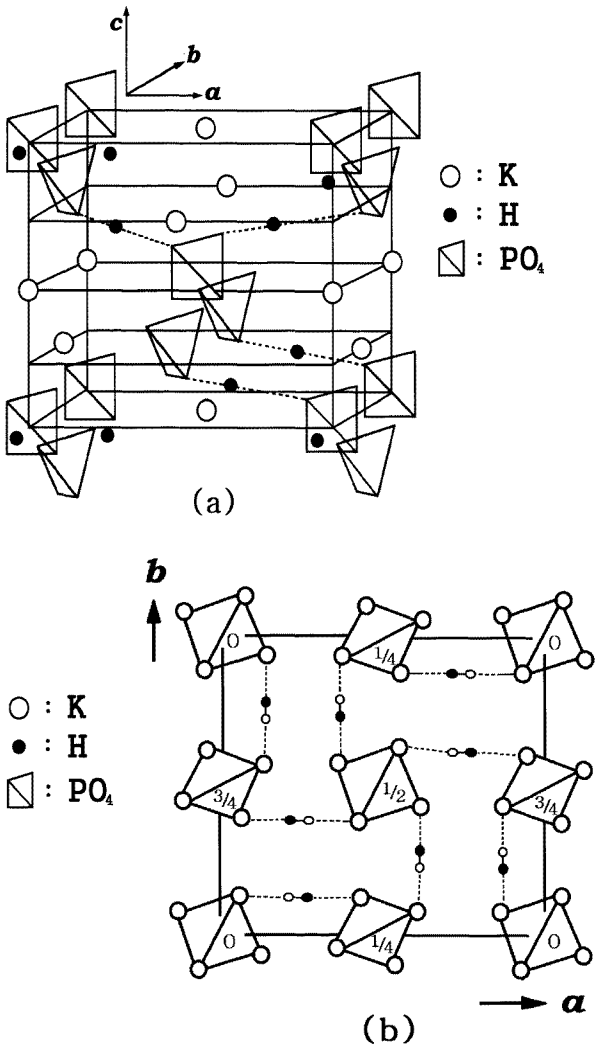

Figure 10. (a) Crystal structure of KH_2PO_4 and RbH_2PO_4 in the paraelectric phase; (b) *c* axis projection of crystal structure. From [1].

the impedance confirms that the model proposed here is appropriate for the description of the high-temperature behaviour of RbH_2PO_4, as in the case of KH_2PO_4 [28]. The temperature dependences of exponents m and n are shown in figure 8. The parameters m and n take values over the entire range $0 \leqslant m, n \leqslant 1$ and may be functions of temperature. The fitting of (10) in the case of the *c* axis always leads to a value of m close to about zero and independent of temperature, but shows a very strong variation of the value of the exponent n. Otherwise, the exponents m and n decrease toward zero near the high-temperature anomaly, but we have not found the limiting value for $m, n = 0$ over the measured temperature range.

The loss peak frequencies, ω_{p1} and ω_{p2}, are obtained by fitting the imaginary impedance data to (10) and the variations of relaxation times $\tau_{c1} = 1/\omega_{p1}$, $\tau_{c2} = 1/\omega_{p2}$ as functions of reciprocal temperature are shown in figure 9. With the exception of the anomalous behaviour in the vicinity of T_p, both τ_{c1} and τ_{c2} decrease upon heating to around 113 °C.

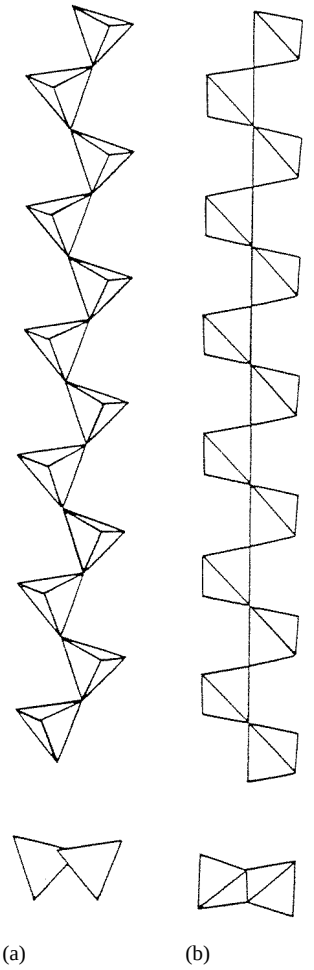

Figure 11. Types of polyphosphate chain configuration. Upper diagrams indicate the relative orientations of adjacent PO_4 tetrahedra extended along the chain axis, and lower diagrams represent projections down these axes: (a) $K_nH_2P_nO_{3n+1}$; (b) $Rb_nH_2P_nO_{3n+1}$. From [23].

The physical origin of impedance relaxations of RbH_2PO_4 at high temperatures can be suggested as in the case of KH_2PO_4 near 180 °C [28]: a fast component in the higher frequency region due to the proton migration in the bulk, and a slow component in the lower frequency region characterized by a formation and migration of H_2O molecules at the surface or electrode/crystal interfacial polarization.

3.4. Structural change at high temperatures

KH_2PO_4 and RbH_2PO_4 crystals have a three-dimensional hydrogen bond network, as shown in figure 10. Below the well-known ferroelectric phase transition temperature T_c, the spontaneous polarization appears along the *c* axis, and the dynamical motion of protons and phonons has been much studied [1]. However, to the authors' knowledge, their surface structure has been little investigated. The reason is that the ferroelectric transition results from the dipole fluctuation in the three-dimensional hydrogen-bond network (figure 10).

The present experimental results show that RbH_2PO_4 near T_p (72–130 °C) exhibits very similar phenomena to KH_2PO_4 near T_p (170–225 °C) and suggest strongly that the high-temperature anomaly of RbH_2PO_4 near T_p may be a partial thermal decomposition at the surface, as demonstrated recently in KH_2PO_4 [14, 28, 29, 30]. The thermal decomposition of solids is, in general, known to begin at the specific localities at or near the surface [26, 31, 32]. Therefore, the weight loss due to the formation of polymers, $Rb_nH_2P_nO_{3n+1}$ with low n, just above T_p may be too small to detect using less sensitive thermogravimetry (TG). A similar surface transformation without appreciable weight loss of bulk has been reported in ferroelastic $(NH_4)_2SO_4$ [34, 35]. However, if we compare the dielectric constant of RbH_2PO_4 (figure 5 in this work) and KH_2PO_4 (figure 1 in [28]) at high temperatures, the very different temperature dependence is noticeable. The remarkable difference at around T_p indicates that the mechanism of the high temperature anomaly of RbH_2PO_4 may be different to that of KH_2PO_4, although they have the same crystal structure (figure 10) at room temperature. The very different temperature dependences of the dielectric constants of RbH_2PO_4 and KH_2PO_4 indicate the formation of different polymeric structures such as $K_nH_2P_nO_{3n+1}$ and $Rb_nH_2P_nO_{3n+1}$, as shown in figure 11.

4. Conclusions

In summary, the high-temperature phenomena observed near T_p in RbH_2PO_4 can be explained as follows. The cracks appeared abruptly near 110 °C, which may be caused by the hydrogen-bond breaking at or near the surface. The DSC shows that the T_p is scattered over the range 82–117 °C according to heating rates. The T_p shifts to lower temperatures as the heating rate increases. The dielectric constant shows a high-temperature anomaly around 113 °C. The present experimental results revealed that the high-temperature anomaly depends strongly on experimental conditions, indicating that the high-temperature phenomenon is controlled by topochemical factors. In the complex ac impedance spectra as a function of temperature and frequency, impedance relaxation was analysed by two Cole–Cole types of relaxation. The fast component may be caused by proton migration, while the slow component may be due to hydrogen-bond breaking and possible polymerization at the surface. As far as the surface of RbH_2PO_4 is concerned, the high-temperature phenomenon of RbH_2PO_4 near T_p is not related to a physical change like the structural phase transition, but related to a chemical change such as thermal decomposition.

Acknowledgments

This work was supported in part by the Korea Science and Engineering Foundation (KOSEF) through the Research Centre for Dielectric and Advanced Matter Physics (RCDAMP) at Pusan National University, and in part by the Basic Science Research Institute Programme, Ministry of Education, Korea, 1997, project No BSRI-97-2411.

Note added in proof. The authors learned quite recently that x-ray diffraction, TG and DSC were used to study the dehydration and the high-temperature transition at T_p in RbH_2PO_4 (Ortiz E, Vargas R A, Cuervo G, Mellander B-E and Gustafson J 1998 *J. Phys. Chem. Solids* **59** 1111). According to this study, the high-temperature transformation at T_p in RbH_2PO_4 is not a bulk structural transition (tetragonal to monoclinic) but a partial formation of the double salt $2RbH_2PO_4{\cdot}Rb_2H_2P_2O_7$, which sets in around T_p at reaction sites on the crystal surface.

References

[1] See, for example, 1987 *Ferroelectrics* **71** and 1987 *Ferroelectrics* **72** (special issues on KH_2PO_4-type ferro- and antiferroelectrics)
[2] Zvorykin A Ya 1963 *Zh. Neorg. Khim.* **8** 274 (1963 *Russ. J. Inorg. Chem.* **8** 138)
[3] Erdey L, Liptay G and Gal S 1965 *Talanta* **12** 883
[4] Blinc R, O'Reilly D E, Peterson E M and Williams J M 1969 *J. Chem. Phys.* **50** 5408
[5] Yaglov V N, Rud'ko P K and Novikov G I 1972 *Izv. Akad. Nauk Beloruss. SSR, Ser. Khim.* **2** 105
[6] D'yakov V A, Koptsik V A, Lebedeva I V, Mishchenko A V and Rashkovich L N 1973 *Kristallografiya* **18** 1227 (1974 *Sov. Phys.–Crystallogr.* **18** 769)
[7] Gallagher P K 1976 *Thermochim. Acta* **14** 131
[8] Rapoport E, Clark J B and Richter P W 1978 *J. Solid State Chem.* **24** 423
[9] Nirsha B M, Gudinitsa E N, Efremov V A, Zhadanov B V, Olikova V A and Fakeev A A 1981 *Zhur. Neorg. Khim.* **26** 2915 (1981 *Russ. J. Inorg. Chem.* **26** 1560)
[10] Baranowski B, Friesel M and Lunden A 1986 *Z. Naturf.* a **41** 981
[11] Baranowski B, Friesel M and Lunden A 1987 *Z. Naturf.* a **42** 565
[12] Baranowski B, Friesel M and Lunden A 1988 *Phys. Scr.* **37** 209
[13] Vargas R A and Torijano E 1993 *Solid State Ion.* **59** 321
[14] Ortiz E, Vargas R A, Mellander B E and Lunden A 1997 *Polish J. Chem.* **71** 1797
[15] Pereverzeva L P, Pogosskaya N Z, Poplavko Yu M, Pakhomov V I, Rez I S and Sil'nitskaya G B 1971 *Fiz. Tverd. Tela* **13** 3199 (1972 *Sov. Phys.–Solid State* **13** 2690)
[16] Grunberg J, Levin S, Pelah I and Gerlich D 1972 *Phys. Status Solidi* b **49** 857
[17] Shapira Y, Levin S, Gerlich D and Szapiro S 1978 *Ferroelectrics* **17** 459
[18] Dalterio R A and Owens F J 1988 *J. Phys. C: Solid State Phys.* **21** 6177
[19] Baranov A I, Khiznichenko V P and Shuvalov L A 1989 *Ferroelectrics* **100** 135
[20] Orlandi D and Simon P 1992 *Ferroelectrics* **125** 455
[21] Seliger J, Zagar V and Blinc R 1993 *Phys. Rev.* B **47** 14753
[22] Colomban Ph and Novak A 1992 *Proton Conductors* ed Ph Colomban (Cambridge: Cambridge University Press) pp 165–82
[23] Thilo E 1962 *Condensed Phosphates and Arsenates in Advances in Inorganic Chemistry and Radiochemistry* vol 4 ed H J Emeleus and A G Sharpe (New York: Academic) pp 1–75
[24] Umegaki T 1989 *Inorganic Phosphate Materials* ed T Kanazawa (Amsterdam: Elsevier) ch 9, p 221
[25] Durif A 1995 *Crystal Chemistry of Condensed Phosphates* (New York: Plenum)
[26] Lee K-S 1996 *J. Phys. Chem. Solids* **57** 333. See many references cited in this paper for the intermediate and final polymers.
[27] de Oliveira A L, de O Damasceno O, de Oliveira J and Schouler E J L 1986 *Mater. Res. Bull.* **21** 877
[28] Park J-H, Lee K-S, Kim J-B and Kim J-N 1996 *J. Phys.: Condens. Matter* **8** 5491
Park J-H, Lee K-S, Kim J-B and Kim J-N 1997 *J. Phys.: Condens. Matter* **9** 9457
[29] Ortiz E, Vargas R A and Mellander B-E 1998 *J. Phys. Chem. Solids* **59** 305
[30] Park J-H, Lee K-S and Kim J-N 1998 *J. Korean Phys. Soc.* (Proc. Suppl.) **32** S1149
[31] Tompkins F C 1976 Decomposition reactions *Treatise on Solid State Chemistry* vol 4 (*Reactivity of Solids*) ed N B Hannay (New York: Plenum) pp 193–231
[32] Brown M E 1988 *Introduction to Thermal Analysis* (London: Chapman and Hall) ch 13
[33] Lee K-S, Park J-H, Kim K-B, Kim J-B and Kim J-N 1997 *J. Phys. Soc. Japan* **66** 1268
[34] Kim J-L and Lee K-S 1996 *J. Phys. Soc. Japan* **65** 2664
[35] Lee K-S, Kim J-L, Jeong H-T and Jeong S-Y 1996 *J. Korean Phys. Soc.* (Proc. Suppl.) **29** S424
[36] Kissinger H E 1957 *Anal. Chem.* **29** 1702
[37] Chem R and Kirsh Y 1981 *Analysis of Thermally Stimulated Processes* (Oxford: Pergamon) pp 92–110
[38] Ozawa T 1965 *Bull. Chem. Soc. Japan* **38** 1881
[39] Jonscher A K 1983 *Dielectric Relaxation in Solids* (London: Chelsea Dielectrics) ch 3
[40] Schmidt V H 1988 *J. Mol. Struct.* **177** 257
Schmidt V H 1988 *Ferroelectrics* **78** 207